12. N. N. Smirnova, "Solution of heat-transfer equations in filtration by the method of reducing the system to an 'equivalent' heat-conduction equation," in: Physical Hydrodynamics and Heat Transfer [in Russian], ITF Sib. Otd. Akad. Nauk SSSR, Novosibirsk (1978), pp. 61-68.
13. I. M. Dzhamalov, "Displacement of petroleum by heat carriers from flooded laminar beds," Neft. Khoz., No. 12, 49-53 (1978).
14. H. S. Carslow and J. C. Jaeger, Conduction of Heat in Solids, Oxford Univ. Press (1959).

COUPLED PROBLEM OF HEAT TRANSFER, HYDRODYNAMICS, AND SOLIDIFICATION IN A MELT

Yu. A. Samoilovich and L. N. Yasnitskii

UDC 536.252

A mathematical model is constructed which describes thermal and hydrodynamic phenomena accompanying the solidification process in a melt. The equations of hydrodynamics take into account viscoelasticity and compressibility of liquid metal. An example of calculations pertaining to solidification of an ingot is given.

Motion of the melt in the still liquid part of a crystallizing ingot greatly affects the quality of the metal product. Many studies have, therefore, been made concerning convective flow in the liquid core of ingots [1-7].

In several studies [1-6] the equations of heat conduction and of melt motion were solved independently of the solidification problem, i.e., for a given configuration and with the interphase boundaries moving according to a given law. In one study [7] a mathematical model has been proposed which, through a coupled formulation of the problems of hydrodynamics, heat transfer, and solidification, accounts for the interdependence between the form of the crystallization front and the mode of thermogravitational convection developing in the liquid phase of the ingot, both varying in time. A numerical simulation of this model [7] is filled with additional difficulties in connection with satisfying the Stefan condition at a movable and generally curvilinear crystallization front. In this study we will supplement the coupled formulation of those problems with the concept of a two-phase zone [8] and will account for the release of the latent heat of crystallization within this zone by stipulating an effective (apparent) specific heat.

In the previous studies [1-7] the flow of liquid steel was calculated through solution of the system of Navier—Stokes equations. At large temperature drops typical of metallurgical processes, the flow of the melt ceases to be laminar, however, and becomes a nonsteady fluctuating one. Under these conditions, moreover, the liquid can exhibit properties not included in the Navier—Stokes law. We propose to replace the Navier—Stokes equations with equations of motion based on the Maxwell law of viscoelasticity and an equation of state of the medium involving a pressure dependence of the density, i.e., accounting for the compressibility of the medium.

In this way the coupled problem of heat transfer, hydrodynamics, and melt solidification is formulated in three segments:

1) problem of heat transfer involving the liquid phase and the solid phase of an ingot and taking into account the release of heat of phase transition within the liquidus—solidus temperature range T_l-T_s;

2) problem of hydrodynamics involving the motion of a compressible viscoelastic liquid in the still unsolidified part of the ingot and taking into account a nonuniform temperature profile as well as the attendant Archimedes body forces;

3) conditions of coupling between the thermal problem and the hydrodynamic problem at the interphase boundary.

Translated from Inzhenerno-Fizicheskii Zhurnal, Vol. 41, No. 6, pp. 1109-1118, December, 1981. Original article submitted January 27, 1981.

0022-0841/81/4106-1377$07.50 © 1982 Plenum Publishing Corporation

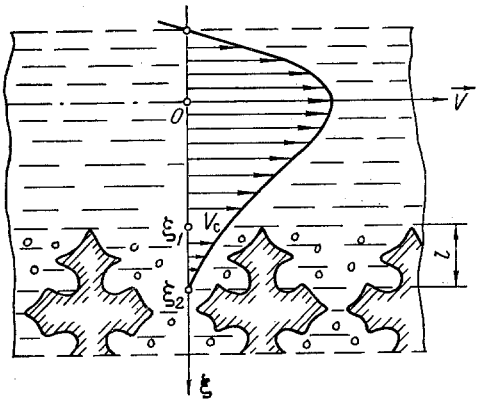

Fig. 1

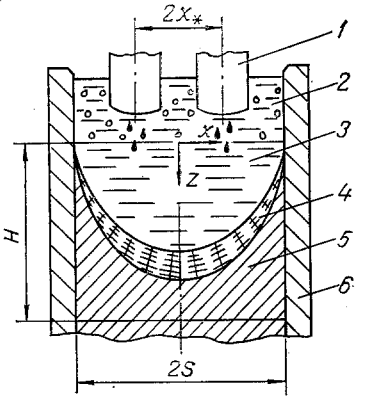

Fig. 2

Fig. 1. Schematic diagram of the velocity profile streamlining the crystallization front.

Fig. 2. Schematic diagram depicting the process of electroslag smelting: 1) fusible electrodes; 2) slag pool; 3) metal pool; 4) two-phase zone; 5) solidified ingot; 6) crystallizer.

The problem of heat transfer in an unsolidified ingot will be formulated on the basis of the equation of transient heat conduction [8]

$$\rho_0 c \frac{dT}{d\tau} = \lambda \nabla^2 T + \rho_0 L \frac{d\Psi}{d\tau}, \tag{1}$$

written in the system of rectangular Cartesian coordinates x, y, z and time τ.

The release of the latent heat of crystallization within the solid—liquid zone is conveniently accounted for by introduction of the effective specific heat $c_{ef}(T)$. For this we let

$$\frac{d\Psi}{d\tau} = \frac{\partial \Psi}{\partial T} \frac{dT}{d\tau} \tag{2}$$

and transform Eq. (1) to

$$\frac{dT}{d\tau} = \frac{\lambda}{\rho_0 c_{ef}(T)} \nabla^2 T. \tag{3}$$

Here

$$c_{ef}(T) = \begin{cases} c_l & \text{at} \quad T > T_l, \\ \dfrac{c_s + c_l}{2} - L \dfrac{\partial \Psi}{\partial T} & \text{at} \quad T_s \leqslant T \leqslant T_l, \\ c_s & \text{at} \quad T < T_s. \end{cases} \tag{4}$$

The dependence of quantity Ψ on the temperature T in the solid—liquid zone was analyzed in an earlier study [9].

We now proceed to derive the appropriate differential equations of motion, regarding the melt in the liquid core of an ingot as a compressible viscoelastic fluid. Accordingly, we write the equation of dynamics for a continuous medium [10] as

$$\rho \frac{d\mathbf{V}}{d\tau} = \rho \mathbf{F} + \operatorname{div} P. \tag{5}$$

We then differentiate Eq. (5) with respect to time and multiply both sides by the constant τ_R characterizing the relaxation time in the medium

$$\tau_R \frac{d\rho}{d\tau} \frac{d\mathbf{V}}{d\tau} + \tau_R \rho \frac{d^2\mathbf{V}}{d\tau^2} = \tau_R \mathbf{F} \frac{d\rho}{d\tau} + \tau_R \frac{d\mathbf{F}}{d\tau} + \operatorname{div}\left(\tau_R \frac{dP}{d\tau}\right). \tag{6}$$

Combining Eqs. (5) and (6), we have

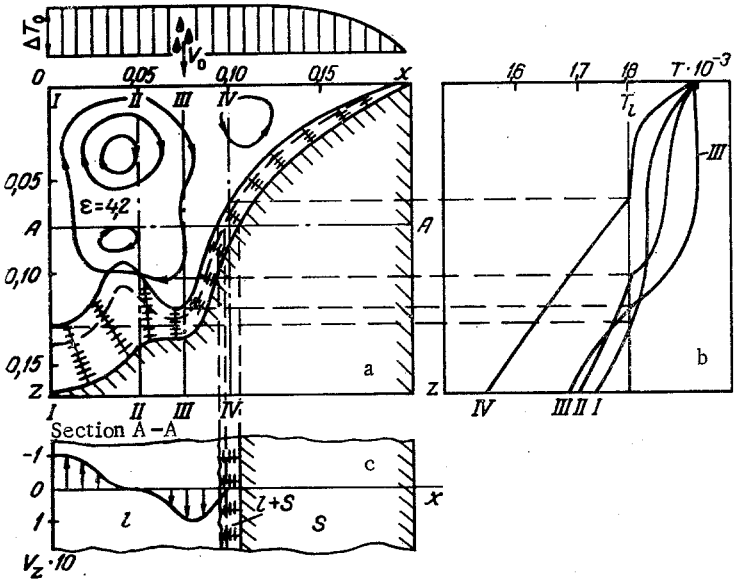

Fig. 3. Field of isotherms in the two-phase zone and of stream lines in the liquid (a), profile of temperature T, °K over pool height in sections I, II, III, IV (b), profile of longitudinal velocity V_z in section A—A (c) for a sheet ingot produced by electroslag smelting with a 120°K superheat of the pool surface and a droplet shower at distance x_* from the ingot axis; x, z, m; $V_z \cdot 10$, m/sec.

$$\rho\left(\frac{d\mathbf{V}}{d\tau}+\tau_R\frac{d^2\mathbf{V}}{d\tau^2}\right)+\tau_R\frac{d\rho}{d\tau}\frac{d\mathbf{V}}{d\tau}=\rho\left(\mathbf{F}+\tau_R\frac{d\mathbf{F}}{d\tau}+\tau_R\mathbf{F}\frac{d\rho}{d\tau}+\operatorname{div}\left(P+\tau_R\frac{dP}{d\tau}\right)\right). \tag{7}$$

The relation between the stress tensor P and the strain rate tensor $\dot{S}$ will be determined from the three-dimensional Maxwell law of rheology written for a compressible isotropic medium

$$P+\tau_R\frac{dP}{d\tau}=2\mu\dot{S}-\left(p+\tau_R\frac{dp}{d\tau}+\frac{2}{3}\mu\operatorname{div}\mathbf{V}\right)E. \tag{8}$$

Inserting expression (8) into Eq. (7) yields

$$\rho\left(\frac{d\mathbf{V}}{d\tau}+\tau_R\frac{d^2\mathbf{V}}{d\tau^2}\right)+\tau_R\frac{d\rho}{d\tau}\frac{d\mathbf{V}}{d\tau}=\rho\left(\mathbf{F}+\tau_R\frac{d\mathbf{F}}{d\tau}\right)+\tau_R\mathbf{F}\frac{d\rho}{d\tau}-\nabla\left(p+\tau_R\frac{dp}{d\tau}\right)+\mu\nabla^2\mathbf{V}+\frac{1}{3}\mu\nabla(\operatorname{div}\mathbf{V}). \tag{9}$$

When the fluid is located in the gravitational force field, then F must be stipulated as the gravitational acceleration **g**. When the density of the fluid is nonuniform in space, owing to a nonuniform temperature distribution, then motion is induced in the fluid which has been called thermogravitational convection. The derivation of well-known equations of thermogravitational convection for an incompressible viscous fluid [11] is based on a linear temperature dependence of the density

$$\rho=\rho_0(1-\beta T), \tag{10}$$

where β is the coefficient of thermal expansion. The pressure dependence of the density has been disregarded here, inasmuch as it is unrelated to the mechanism of thermogravitational convection [11]. Inserting expression (10) into Eq. (9) and considering that nonuniformity of the melt density is taken into account only in determination of the lift force (as in the Boussinesq approximation [11]), we obtain the equation of motion for a viscoelastic fluid in the gravitational force field

$$\frac{d\mathbf{V}}{d\tau}+\tau_R\frac{d^2\mathbf{V}}{d\tau^2}=\mathbf{g}(1-\beta T)-\tau_R\mathbf{g}\beta\frac{dT}{d\tau}-\frac{1}{\rho_0}\nabla\left(p+\tau_R\frac{dp}{d\tau}\right)+\nu\nabla^2\mathbf{V}+\frac{1}{3}\nu\nabla(\operatorname{div}\mathbf{V}). \tag{11}$$

We can reduce the order of the differential Eq. (11) by introducing the concept of fluid acceleration W:

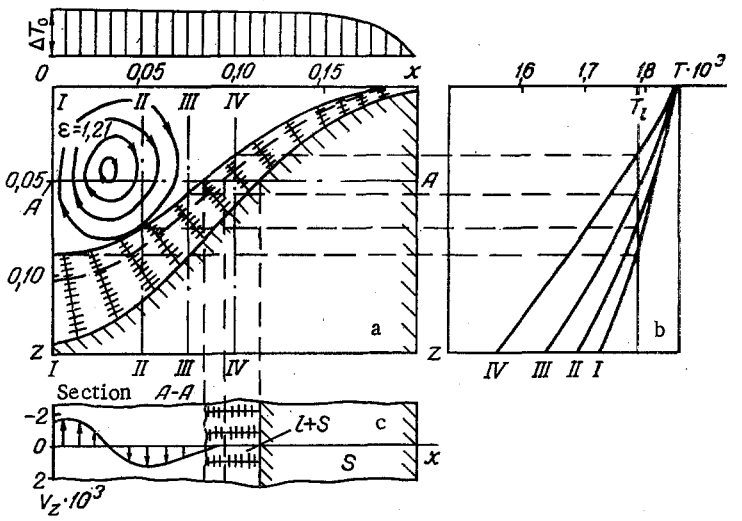

Fig. 4. Field of isotherms in the two-phase zone and of stream lines in the liquid (a), profile of temperature T, °K over pool height in sections I, II, III, IV (b), profile of longitudinal velocity V_z, m/sec in section A—A (c) for a sheet ingot produced by electroslag smelting with a 70°K superheat of the pool surface.

$$\mathbf{W} = \frac{d\mathbf{V}}{d\tau}, \tag{12}$$

so that

$$\tau_R \frac{d\mathbf{W}}{d\tau} + \mathbf{W} = (1 - \beta T)\,\mathbf{g} - \tau_R\, \mathbf{g}\beta \frac{dT}{d\tau} - \frac{1}{\rho_0} \nabla p - \frac{\tau_R}{\rho_0} \nabla \frac{dp}{d\tau} + \nu \nabla^2 \mathbf{V} + \frac{\nu}{3} \nabla \operatorname{div} \mathbf{V}, \quad \nu = \mu/\rho_0. \tag{13}$$

In order to close the system of equations, it is necessary to add the equation of continuity

$$\frac{\partial \rho}{\partial \tau} + \operatorname{div}(\rho \mathbf{V}) = 0 \tag{14}$$

and the equation of state for a compressible fluid

$$\rho = \rho_0 (1 + \alpha p). \tag{15}$$

They combine into the single equation

$$\frac{dp}{d\tau} = -\left(p + \frac{1}{\alpha}\right) \operatorname{div} \mathbf{V}. \tag{16}$$

The equation of motion (13) can be transformed with the aid of Eqs. (3) and (16), viz.

$$\tau_R \frac{d\mathbf{W}}{d\tau} + \mathbf{W} = (1 - \beta T)\,\mathbf{g} - \frac{\tau_R\, \mathbf{g}\beta\lambda}{\rho_0 c_{\text{ef}}(T)} \nabla^2 T - \frac{1}{\rho_0} \nabla p + \frac{\tau_R}{\rho_0} \nabla (p \operatorname{div} \mathbf{V}) + \left(\frac{\tau_R}{\rho_0 \alpha} + \frac{\nu}{3}\right) \nabla \operatorname{div} \mathbf{V} + \nu \nabla^2 \mathbf{V}. \tag{17}$$

We now resolve the total derivatives with respect to time into their local and convective parts, whereupon we reduce the resulting system of equations to dimensionless form. We select the characteristic linear dimension of the integration region S as the unit of distance measurement, S^2/ν for time, ν/S for velocity, ν^2/S^3 for acceleration, ΔT_0 for temperature, and $\rho_0 \nu^2/S^2$ for pressure so that

$$\frac{\partial \mathbf{W}}{\partial \tau} + (\mathbf{V}\nabla)\,\mathbf{W} = -\frac{1}{N_{Rs}}\,\mathbf{W} + \gamma \frac{N_{Gr}}{N_{Rs}}\,T + \gamma \frac{N_{Gr}}{N_{Pr}} \nabla^2 T - \frac{1}{N_{Rs}} \nabla p$$
$$+ \nabla (p \operatorname{div} \mathbf{V}) + \left(\frac{1}{N_J} + \frac{1}{3N_{Rs}}\right) \nabla \operatorname{div} \mathbf{V} + \frac{1}{N_{Rs}} \nabla^2 \mathbf{V} - \gamma \frac{N_{Gr}}{N_{Rs}}, \tag{18}$$

$$\frac{\partial \mathbf{V}}{\partial \tau} + (\mathbf{V}\nabla)\,\mathbf{V} = \mathbf{W}, \tag{19}$$

$$\frac{\partial T}{\partial \tau} + \mathbf{V}\nabla T = \frac{1}{N_{Pr}}\,\nabla^2 T, \tag{20}$$

$$\frac{\partial p}{\partial \tau} + \mathbf{V}\nabla p = -\left(p + \frac{1}{N_J}\right)\operatorname{div}\mathbf{V}. \tag{21}$$

Equations (18)-(21) have been written in dimensionless velocity, acceleration, temperature, and pressure and all derivatives have been taken with respect to dimensionless space coordinates and time.

This system of equations (18)-(21) describing the behavior of a compressible viscoelastic fluid in the gravitational force field contains five dimensionless parameters: Grashof number $N_{Gr} = g\beta\Delta T_0 S^3/\nu^2$, Galileo number $N_{Ga} = gS^3/\nu^2$, Prandtl number $N_{Pr} = \nu\rho_0 c_{ef}(T)/\lambda$, and $N_J = \alpha\rho_0\nu^2/S^2$, $N_{RS} = \tau_R\nu/S^2$ which can be called compressibility number and relaxation number, respectively. We note that with the last two numbers equal to zero the system of equations (18)-(21) reduces to the conventional Boussinesq approximation describing the thermogravitational convection in an incompressible viscous fluid [11].

We now supplement the system of equations (18)-(21) with the condition of "stagnation"

$$\mathbf{V} = 0, \quad \mathbf{W} = 0 \quad \text{at} \quad T \leqslant T_E \tag{22}$$

and the boundary condition at the interface between the two-phase zone and the stream of melt flowing along the crystallization front [2]

$$V + l\,\frac{\partial V}{\partial \xi} = 0 \quad \text{at} \quad T = T_l. \tag{23}$$

This boundary condition generalizes the boundary condition of adhesion and reflects the effect of a dendrite structure of the crystallization front on the velocity profile in the boundary layer. The velocity profile V near the crystallization front is shown schematically in Fig. 1, where the dimension l denotes the depth of the part of the solid—liquid transition zone dragged by the stream. Condition (23), moreover, is satisfied by a linear velocity profile

$$V = V_c\left(1 - \frac{\xi - \xi_1}{l}\right).$$

The thickness l of the drag layer is defined as the distance between the liquidus isotherm ($T = T_l$) and the pourability isotherm ($T = T_E$), as it pertains to the solution of the heat-conduction problem.

The algorithm of the solution is constructed so that Eqs. (18)-(21) are simultaneously solved over the entire region of concern (encompassing the solid zone and the liquid zone as well as the transition zone), but condition (22) is satisfied on each time step by equating the velocity and the acceleration in the solid part of the ingot ($T \leq T_E$) to zero (stagnation). Condition (23) accounts for the effect of a dendrite structure of the crystallization front, viz. a lower velocity of liquid metal within the two-phase zone of a solidifying ingot.

Here is an example of using this method, with $N_J = 0$ and $N_{RS} = 0$ as a special case, for mathematical simulation of the ingot solidification process in a bifilar-type electroslag smelting furnace [12]. The basic scheme for producing a flat ingot of thickness $2S = 0.4$ m by the method of electroslag smelting is shown in Fig. 2. The origin of the moving system of coordinates has been placed at the center of the free surface of the melt in the metal pool and the z axis has been directed downward along the ingot axis. For calculations is selected the right-hand half of the ingot, bounded at the top by the free surface of the melt and at the bottom by the horizontal plane at the distance $H = 0.3$ m from the origin of coordinates.

The boundary conditions for the problem of producing an ingot by electroslag smelting are more conveniently put in a dimensional form. At the surface of the metal pool we assume a temperature distribution

$$T = T_E + \Delta T_0\,[1 - (x/S)^m] \quad \text{at} \quad z = 0, \tag{24}$$

where $\Delta T_0 = \text{const}$ is the maximum temperature drop across the free surface of the melt and $m = \text{const}$ is a power exponent ranging from 2 to 10.

At the lateral surface of the ingot we use the Newton—Rikhman boundary condition

$$-\lambda \left.\frac{\partial T}{\partial x}\right|_{x=S} = K_{ing}(T_{sur} - T_{cool}), \tag{25}$$

and at its axis we use the condition of a symmetric temperature profile

$$\frac{\partial T}{\partial x} = 0 \quad \text{at} \quad x = 0, \tag{26}$$

while at the bottom section we use the so-called condition of ingot extendability (condition of thermal contact with the fictitiously discarded lower part of the ingot)

$$\frac{\partial^2 T}{\partial z^2} = 0 \quad \text{at} \quad z = H. \tag{27}$$

The boundary conditions for the velocity and acceleration field at the surface of the metal pool follow from the hypothetical absence of viscous friction forces here and also from the assumption that the slag—metal boundary remains plane, viz.

$$\frac{\partial V_x}{\partial z} = 0, \quad V_z = 0, \quad \frac{\partial W_x}{\partial z} = 0, \quad W_z = 0 \quad \text{at} \quad z = 0. \tag{28}$$

At the ingot axis we stipulate symmetry of the velocity profile and the acceleration profile

$$V_x = 0, \quad \frac{\partial V_z}{\partial x} = 0, \quad W_x = 0, \quad \frac{\partial W_z}{\partial x} = 0 \quad \text{at} \quad x = 0. \tag{29}$$

The pressure distribution over the boundaries of the region selected for calculations depends on the overall pattern of motion and should be determined during solution of the hydrodynamic problem. From this standpoint, we find applicable the condition of a zero normal derivative of pressure at all boundaries of this region

$$\frac{\partial p}{\partial n} = 0. \tag{30}$$

The shower of droplets falling from the fusible electrodes on the surface of the metal pool is distributed over some area of that surface. One can reasonably assume that the region of maximum shower intensity stretches along the axis of the electrodes and thus at a distance x_* from the plane of symmetry of the ingot (Fig. 2). On the basis of data obtained by observation of droplets passing into the melt [13-15], one can approximately describe the attenuation of the vertical velocity component V_Z by the exponential relation

$$V_z = V_0 \exp\left(-\eta \frac{z}{H_м}\right) \quad \text{at} \quad x = x_*. \tag{31}$$

For a numerical solution of the problem on the basis of this mathematical model, we used the method of finite elements [16] together with a technique of smoothing in space and averaging in time analogous to the technique used in another study [17].

The results of such a simulation of the steady-state mode of casting by electroslag smelting with an initial fusion rate of $0.5 \cdot 10^{-4}$ m/sec are shown in Fig. 3 in the form of the field of liquid-metal stream lines, of the two-phase zone, of the temperature field and the velocity field in ingot sections. For the calculations, the following empirical constants and physical characteristics of carbon steel were used: $\Delta T_0 = 120°K$, $m = 5$, $K_{ing} = 500$ W/(m^2·K), $T_{cool} = 300°K$, $x_* = 3/8$ S, $\eta = 1.25$, $V_0 = 0.15$ m/sec, $T_l = 1783°K$, $T_S = 1733°K$, $T_E = 1773°K$ (this pourability temperature corresponds to the state of the metal in which an elementary volume within the two-phase zone contains 30% solid phase: $\Psi = 0.3$), $\rho_0 = 7 \cdot 10^3$ kg/m^3, $c_S = 600$ J/(kg·K), $c_l = 800$ J/(kg·K), $\lambda = 29$ W/(m·K), $\beta = 0.17 \cdot 10^{-3}$ K^{-1}, $L = 272{,}000$ J/kg, and $\nu = 0.6 \cdot 10^{-6}$ m^2/sec.

The diagram in Fig. 3 indicates that circulation of the melt in the metal pool has resulted in a noticeable nonuniformity of the temperature distribution over an ingot section. While in section I (along the ingot axis $x = 0$) most of the metal superheat relaxes at the upper horizontals in the metal pool, in section III (along the electrode axis $x = x_*$) the

superheated metal spreads rather deeply. The diagram in Fig. 3 also shows a cavity produced at the bottom of the metal pool by the heat which the droplet shower carries from the free surface deeper into the melt.

The diagram in Fig. 4 shows the results of simulation of thermogravitational convection in the melt ($\Delta T_0 = 70°K$) which can occur in the metal pool of the ingot during the final stage of the electroslag smelting process, when the droplet shower has already ceased (condition (17) is not used in the simulation) but the liquid lune has not yet solidified. The weak convection streams produced here by Archimedes body forces, unlike those in the preceding case, have no noticeable effect whatsoever on the temperature field of the metal pool.

In the course of calculations the local temperature gradients in the metal at various points of the pool were determined, with and without convection taken into account, whereupon the ratio $\varepsilon = \lambda_{eff}/\lambda$ was calculated (λ_{eff} denoting the so-called effective thermal conductivity generally used for simplified engineering calculations and characterizing the increase of thermal conductivity of the melt due to intense stirring, and λ denoting the molecular thermal conductivity of the melt). According to the calculations, $\varepsilon \simeq 1.2$ in the case of thermogravitational convection and $\varepsilon \simeq 4.2$ in the case of forced circulation of the melt by action of a droplet shower.

Formulation and solution of the coupled problem of heat transfer, hydrodynamics, and solidification thus makes it possible to calculate temperature and hydrodynamic fields taking their interdependence into account, and to predict the form of the crystallization front depending on the degrees of superheat of the free surface and on the intensity of circulation of liquid metal in the unsolidified part of the ingot.

NOTATION

x, y, z, rectangular Cartesian coordinates; τ, time; V, velocity vector with components V_x, V_y, V_z; $\mathbf{W}$, acceleration vector with components W_x, W_y, W_z; ρ, density of the medium; ρ_0, density of the medium at temperature T_0 and under pressure p_0; T, temperature defined as the difference between the actual temperature and the initial temperature T_0; p, pressure defined as the difference between the actual pressure and the initial pressure p_0; $\Psi = Q_s/Q$, relative amount of solid phase; Q_s, volume of solid phase contained in an elementary volume Q; T_l, liquidus temperature; T_s, solidus temperature; T_E, pourability temperature, corresponding to the state in which the two-phase zone contains a definite amount of solid phase (e.g., $\Psi = 0.3$); c, specific heat; λ, thermal conductivity; μ, dynamic viscosity; ν, kinematic viscosity; L, specific heat of crystallization; c_{ef}, effective specific heat; c_l, specific heat of the liquid phase; c_s, specific heat of the solid phase; F, density of body force distribution; P, stress tensor; S, strain tensor; τ_R, relaxation time; E, tensor unit; g, gravitational acceleration; β, coefficient of thermal expansion; α, isothermal compressibility factor; $2S$ and H, width and the height of the region selected for calculations; ΔT_0, maximum temperature drop; γ, unit vector in the upward vertical direction; N_{Gr}, Grashof number; N_{Ga}, Galileo number; N_{Pr}, Prandtl number; N_J, compressibility number; N_{Rs}, relaxation number; T_{cool}, temperature of the medium cooling the crystallizer; K_{ing}, heat-transfer coefficient at the lateral surface of the ingot; $T_{sur} = T(S, z)$, temperature of the lateral surface of the ingot; η, a coefficient characterizing the penetration depth of droplets in the melt; H_M, depth of the metal pool; $2x_*$, distance between electrodes; V_0, initial velocity of droplets; and $\varepsilon = \lambda_{eff}/\lambda$, ratio of effective to molecular thermal conductivity.

LITERATURE CITED

1. É. A. Iodko, "Calculation of convection streams in the liquid core of solidifying bodies of simplest shape," Inzh.-Fiz. Zh., 10, No. 1, 92-100 (1966).
2. Yu. A. Samoilovich, "Hydrodynamic phenomena in the unsolidified part (liquid core) of an ingot," Izv. Akad. Nauk SSSR, Met., No. 2, 84-92 (1969).
3. B. I. Vaisman and E. L. Tarunin, "Effect of crystallization on process of natural convection in molten metals," Scientific Notes, Perm Univ., No. 293, 107-118 (1972).
4. P. F. Zavgorodnii, I. L. Povkh, G. M. Sevost'yanov, and N. S. Sidel'nikova, "Asymmetry of thermogravitational convection," Inzh.-Fiz. Zh., 32, No. 1, 102-108 (1977).
5. J. Sheckly and A. G. Dilavari, "Mathematical description of heat and mass transfer phenomena during electroslag refining," in: Problems in Special-Purpose Electrometallurgy (Proc. of Soviet—American Symp.), Kiev (1979), pp. 45-65.

6. P. G. Kroeger and S. Ostrach, "Solution of the two-dimensional problem of freezing with inclusion of convectional effects in the liquid region," Int. J. Heat Mass Transfer, 17, No. 10, 1191-1207 (1974).
7. B. I. Myznikova and E. L. Tarunin, "Natural convection in molten metals during crystallization," in: Mathematical Methods of Analyzing the Processes of Special-Purpose Electrometallurgy [in Russian], Kiev (1976), pp. 129-136.
8. Yu. A. Samoilovich, Ingot Forming [in Russian], Metallurgiya, Moscow (1977).
9. Yu. A. Samoilovich and E. A. Chesnitskaya, "Approximate analytical method of calculating the solidification of ingots," Tr. Vsesoyuz. Nauch.-Issled. Inst. Metallurg. Teplotekh., No. 17, 97-118 (1967).
10. L. G. Loitsyanskii, Mechanics of Liquids and Gases [in Russian], Nauka, Moscow (1978).
11. G. Z. Gershuni and E. M. Zhukhovitskii, Convective Stability of Incompressible Fluids, Halsted Press (1976).
12. B. I. Medovar, L. M. Stupak, G. A. Boiko, et al., Electroslag Furnaces (B. E. Paton and B. I. Medovar, editors) [in Russian], Naukova Dumka, Kiev (1976).
13. V. V. Panin, O. B. Borovskii, I. S. Ivakhnenko, and S. A. Iodkovskii, "X-ray study of steel smelting by the electroslag process," Izv. Akad. Nauk SSSR, Metall. Gornoe Delo, No. 6, 90-95 (1963).
14. V. V. Panin, O. B. Borovskii, I. S. Ivakhnenko, and S. A. Iodkovskii, "Behavior of droplets and of surface of liquid-metal pool during electroslag smelting," Avtomat. Svarka, No. 2, 72-74 (1964).
15. D. A. Dudko, G. Z. Voloshkevich, I. I. Sumuk-Slyusarenko, and I. I. Lychko, "Study of the electroslag process by means of kinematography and photography through a translucent medium," Avtomat. Svarka, No. 2, 15-17 (1971).
16. Ya. A. Samoilovich and L. N. Yasnitskii, "Algorithm of solution of problems in thermogravitational convection of incompressible viscous fluid by the method of finite elements," Tr. Permsk. Univ. (manuscript No. 1131-80 deposited at All-Union Institute of Scientific and Technical Information March 24, 1980).
17. A. G. Daikovskii, V. I. Polezhaev, and A. I. Fedoseev, "Numerical simulation of transitional and turbulent modes of flow on the basis of transient Navier—Stokes equations," Preprint, Inst. Prikl. Mekh., Akad. Nauk SSSR, No. 101 (1978).

ONE APPROACH TO SOLVING REVERSE PROBLEMS OF HEAT CONDUCTION

Yu. M. Matsevityi

UDC 536.24

Ways are proposed to identify the thermophysical parameters in nonstandard situations (heat transfer in the case low external thermal resistances, thermal conductivity of thin coatings).

The class of reverse problems of heat conduction is rather large, it includes external or boundary problems (determination of boundary conditions from the known mathematical model and available data on the temperature field in the given object), internal or coefficient problems (identification of thermophysical characteristics from available data on the boundary conditions and the temperature field), geometrical problems (determination of the geometrical characteristics of a thermal object), model or inductive problems (refinement of the mathematical model), and finally time or retrospective problems where the initial or simply earlier thermal state is to be determined from available data on the process at later instants of time.

The need to formulate these problems arises from the great difficulties encountered in experimental determination of aforementioned thermophysical parameters and by a natural desire to utilize methods of mathematical simulation for their identification.

Institute of Problems in Machine Design, Academy of Sciences of the Ukrainian SSR, Kharkov. Translated from Inzhenerno-Fizicheskii Zhurnal, Vol. 41, No. 6, pp. 1119-1123, December, 1981. Original article submitted September 16, 1980.

 0022-0841/81/4106-1384$07.50 © 1982 Plenum Publishing Corporation